Adaptive OFDM for wideband radio channels

Andreas Czylwik

Deutsche Telekom AG, Research Center
Am Kavalleriesand 3, 64295 Darmstadt, Germany
Tel.: +49-6151-83-3537, Fax: +49-6151-83-4638, E-Mail: czylwik@fz.telekom.de

Abstract

An OFDM (orthogonal frequency division multiplexing) transmission system is simulated with time-variant transfer functions measured with a wideband channel sounder. The individual subcarriers are modulated with fixed and adaptive signal alphabets. Furthermore, a frequency-independent as well as the optimum power distribution are used.

The simulations show that with adaptive OFDM, the required signal power for an error probability of 10^{-3} can be reduced by 5 ... 15 dB compared with fixed OFDM. The fraction of channel capacity which can be achieved with adaptive OFDM depends on the average signal-to-noise ratio and the propagation scenario.

1 Introduction

Shannon has shown that, theoretically, it is possible to transmit information over a given channel with an arbitrary small error probability if the data rate is not greater than the channel capacity (information rate). Therefore, the channel capacity is the ultimate limit of the data rate for reliable communication. In the present contribution the channel capacity of a wideband radio channel with fixed antennas and with frequency-selective fading is compared with the achieveable data rate using adaptive orthogonal frequency division multiplexing (OFDM) transmission schemes. Radio channels with frequency-selective fading originate from multipath propagation and can be found in broadband wireless local area networks (LANs) or broadband wireless access networks.

In an OFDM transmission system which uses the same fixed modulation scheme for all OFDM subcarriers, the error probability is dominated by the OFDM subcarriers with highest attenuation. Therefore, in case of frequency-selective fading the error probability decreases very slowly with increasing average signal-to-noise ratio (SNR). This problem can be mitigated if different modulation schemes are employed for the individual OFDM subcarriers. The modulation schemes have to be adapted to the SNRs of the individual subcarriers. Furthermore, the power distribution for the individual subcarriers can be optimized. In the present contribution only uncoded modulation schemes are considered.

In order to combat the temporal fluctuations of a radio channel, adaptive single carrier modulation schemes are proposed in literature [1, 2]. Also in the field of OFDM, adaptive channel usage is recommended [3]. Adaptive OFDM based on the optimum water-pouring method is well-known in the field of transmission over twisted-pair lines [4, 5, 6]. But in the field of multipath radio channels, the water-pouring method with variable modulation schemes is considered only sparcely [7]. Therefore, in the present paper the performance of adaptive OFDM in a radio system is investigated in detail.

The paper is organized as follows: In section 2 the channel capacity of a measured broadband radio channel is calculated and in section 3 transmission systems with adaptive OFDM are presented. Finally, section 4 contains simulation results.

2 Channel capacity

The channel capacity of an ideal transmission channel with additive white Gaussian noise (AWGN) can be calculated using Shannons formula [8]:

$$C = B \cdot \mathrm{ld}\left(1 + \frac{P_x}{P_n}\right), \tag{1}$$

where B denotes the (single-sided) channel bandwidth, P_x the average signal power and P_n the average noise power in the bandwidth B. Equation (1) shows that the channel capacity only depends on the bandwidth B and on the signal-to-noise ratio ($\mathrm{SNR} = P_x/P_n$). In case of a frequency-selective channel the capacity is determined by the ratio of the signal's power spectral density (PSD) $S_x(\omega)$ to the noise PSD $S_n(\omega)$. The transmission channel has to be divided into a large number of narrowband subchannels where the transfer function can be considered as constant. The channel capacity results from integration over all subchannels [9, 10]:

$$C = \frac{1}{2\pi}\int_0^\infty \mathrm{ld}\left(1 + \frac{S_x(\omega)}{S_n(\omega)}\right) \mathrm{d}\omega. \tag{2}$$

The integrand in Eq. (2)

$$C' = \mathrm{ld}\left(1 + \frac{S_x(\omega)}{S_n(\omega)}\right) \tag{3}$$

will be called the density of the channel capacity. C' determines the maximum data rate per bandwidth. Therefore, it is the ultimate limitation of bandwidth efficiency. Its unit is $\frac{\mathrm{bit/s}}{\mathrm{Hz}} = \mathrm{bit}$.

It is assumed that the transmitted signal is limited by its mean power P_x. In this case the maximum of channel capacity is obtained if the PSD of the transmitted signal $S_x(\omega)$ is adapted to the transfer function of the channel. The optimum method for distribution of power is the well-known "water-pouring" method [10]:

$$S_{x_{\mathrm{opt}}}(\omega) = \begin{cases} S_{\mathrm{max}} - S_n(\omega) & \text{for} \quad S_{\mathrm{max}} - S_n(\omega) \geq 0 \\ 0 & \text{else.} \end{cases} \tag{4}$$

The parameter S_{max} has to be chosen such that the boundary condition

$$P_x = \frac{1}{\pi}\int_0^\infty S_x(\omega)\,\mathrm{d}\omega \tag{5}$$

is fulfilled.

A radio channel is described by a time-variant transfer function $H(t,\omega)$ [11] and an additive white Gaussian noise (AWGN) source (thermal noise $n_{\text{th}}(t)$). The corresponding block diagram is shown in Fig. 1. Because of the time-variant behaviour, the channel capacity changes with time, too. Propagation measurements of radio channels with fixed antennas show that the transfer function varies very slowly with time. Because of this reason it is assumed that the instantaneous transfer function of the radio channel can be estimated at the receiver and can be communicated back to the transmitter via signalling channels with noticable delay. Therefore, only in a bidirectional transmission system, the transmitted power spectrum can be optimized.

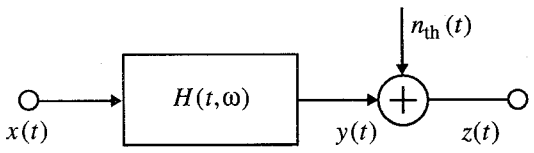

Figure 1: Block diagram of a time-variant radio channel.

The power spectral density of the equivalent input noise of a time-variant radio channel is given by:

$$S_n(t,\omega) = \frac{k\,T_0}{2} \cdot F \cdot \frac{1}{|H(t,\omega)|^2} \qquad (6)$$

where F denotes the noise figure, k Boltzmann's constant, and T_0 the reference temperature. Since the equivalent input noise is time-variant, also the optimum PSD $S_{x_{\text{opt}}}(\omega)$ and the channel capacity become time-variant.

From a qualitative point of view, with the water-pouring method, most of the power is concentrated in frequency ranges where the channel attenuation is small. Numerical evaluations of channel capacity have shown that there is only a very small loss of channel capacity if a white power spectrum is used instead of the optimum power spectrum [12]. This result holds for the case that the average SNR is high. Only in case of a low average SNR, the channel capacity can be increased significantly with an optimized power spectrum. Therefore, only the case of a frequency-independent signal power spectrum is considered for the calculation of channel capacity.

For the numerical evaluation, data from wideband outdoor propagation measurements in an industrial area in Darmstadt, Germany, were used. The measurements were carried out with fixed antennas. The transfer function of a first propagation measurement with two omni-directional antennas and under line-of-sight (LOS) conditions is displayed in Fig. 2a. In a second measurement an omni-directional and a sectional antenna (angle of aperture: 110°) were used. The omni-directional antenna was located inside a building so that there were non-line-of-sight (NLOS) conditions. The most important parameters of both measurement scenarios are summarized in Table 1.

The channel capacity was evaluated within a bandwidth of $B = 5$ MHz. The resulting temporal fluctuations of channel capacity are shown in Fig. 3 (The channel capacity is normalized with the bandwidth B: $\overline{C'} = C/B$). The level of transmitted power was adjusted so that for both measurements a similar average SNR results. The curves show that the fluctuations in the LOS case are much stronger than in

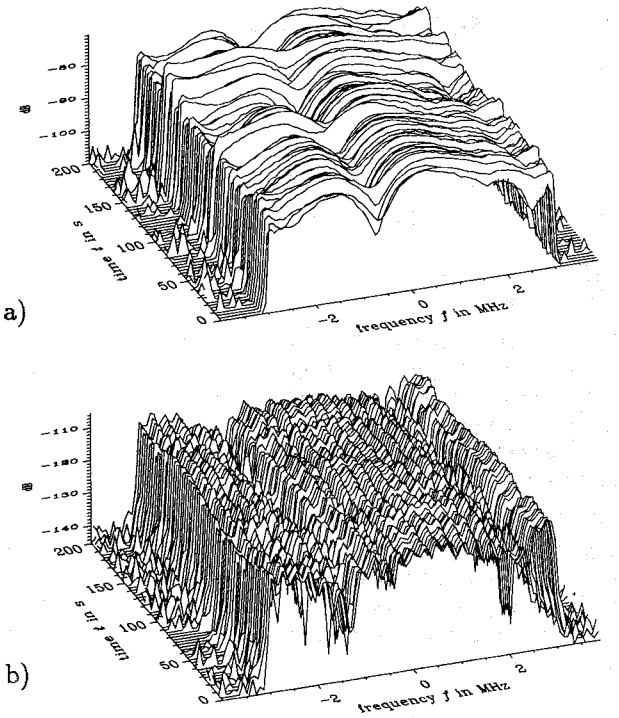

Figure 2: Time-variant transfer function of measurement 1 (a) and measurement 2 (b).

	measurement 1	measurement 2
distance of antennas	95 m	230 m
carrier frequency	1.8 GHz	
bandwidth of measurement	6 MHz	
average attenuation $-10\lg(\langle\|H(t,\omega)\|^2\rangle)$	77.4 dB	112.0 dB
delay-spread	0.31 μs	1.15 μs

Table 1: Parameters of the propagation scenarios.

the NLOS case. This is due to the stronger correlation of the transfer function at different frequencies in the LOS case.

The fluctuations of the overall channel capacity are much smaller than the fluctuations of capacity in individual subchannels. This is caused by the fact that frequency-selective fluctuations compensate each other to some extent.

3 Adaptive OFDM transmission

The block diagram of the considered OFDM transmission system is sketched in Fig. 4. The bit stream of a binary source is fed to an adaptive modulator which generates complex symbols on its output. The modulator adapts the signal alphabets (and the average powers) of the individual OFDM subcarriers to the transfer function at the respective frequencies. In the following block, the complex symbols are transformed with an inverse fast Fourier transform (FFT) into time domain. The number of subcarriers (length of FFT vectors) is denoted with n_{FFT}. Next, a cyclic extension (guard interval) is added which reduces interblock interference. The output signal is transmitted over the radio channel which is represented by a time-variant linear filter and an AWGN channel. A complex baseband description of the radio channel is used. At the receiver the cyclic extension is removed and the signal is transformed back into frequency domain with an FFT. Prior

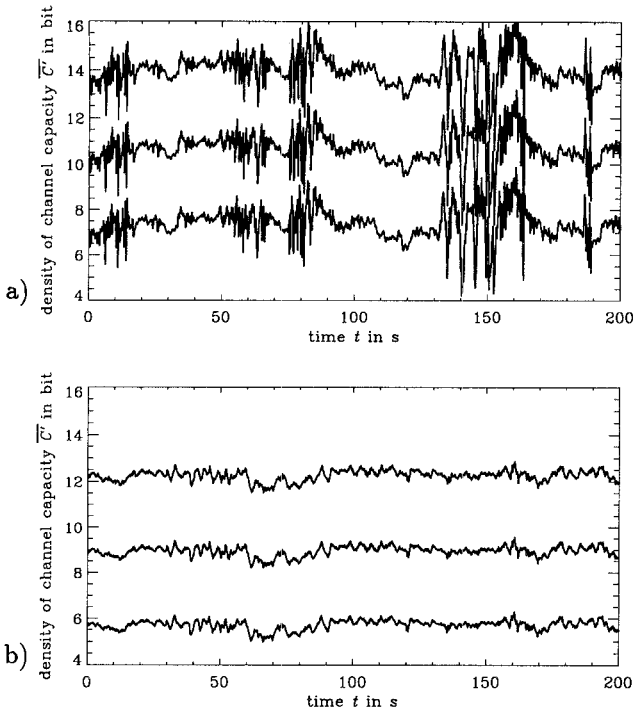

Figure 3: Temporal fluctuation of the normalized channel capacity $\overline{C'} = C/B$ for a) measurement 1 and b) measurement 2. $\overline{C'}$ is the average density of channel capacity with respect to frequency for the bandwidth $B = 5$ MHz. Transmitted power: a) 0 dBm, 10 dBm, 20 dBm; b) 30 dBm, 40 dBm, 50 dBm.

to demodulation, the signal is equalized in frequency domain with the inverse of the transfer function. Finally, an adaptive demodulator detects the transmitted symbols and generates the output bit stream.

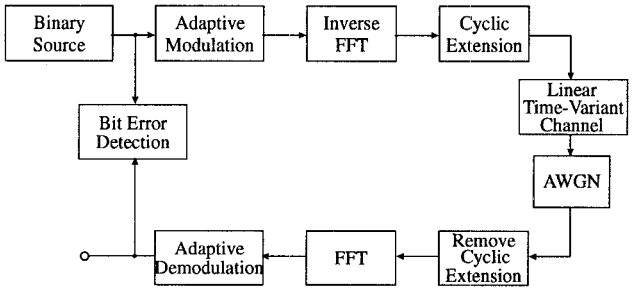

Figure 4: Block diagram of an OFDM transmission system.

The temporal variation of the transfer function of a radio channel makes it necessary to adapt the modulation schemes of the transmitted subcarriers continuously. The adaptive modulator and demodulator have to be synchronized via a signalling channel which is disregarded in the present contribution. Furthermore, ideal carrier and clock recovery are assumed.

The input signal of the adaptive modulator is processed blockwise due to the blockwise signal processing of the FFT blocks. For most applications of broadband radio systems a constant data rate is required. Therefore, also the adaptive modulator has to transmit with a constant data rate. This means that with each FFT block the same number of bits M is transmitted. Two different modulator/demodulator pairs are considered. In modulator A, the distribution of bits to the individual subcarriers is adapted to the shape of the transfer function of the radio channel. Modulator B optimizes simultaneously the distribution of bits and the distribution of signal power with respect to frequency. The algorithms for the distribution of bits and power are described later in this section.

Different QAM modulation formats can be selected: no modulation, 2-PSK, 4-PSK, 8-QAM, 16-QAM, 32-QAM, 64-QAM, 128-QAM, and 256-QAM (see Fig. 5). This means that 0, 1, 2, 3, ... 8 bit per subcarrier and FFT block can be transmitted. In order to get a minimum overall error probability, the error probabilities for all used carriers should be approximately equal.

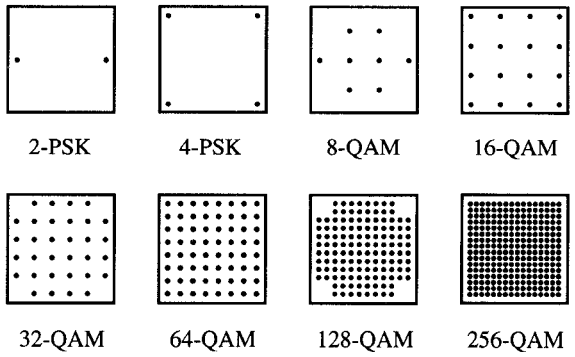

Figure 5: Constellation diagrams of the used QAM schemes.

The required SNR for the above mentioned modulation schemes is displayed in Fig. 6 for given symbol error probabilities. Using Gray coding, the bit error probability is approximately equal to the symbol error probability. The figure shows the bandwidth efficiency of different modulation schemes as a function of SNR. It is obvious that the bandwidth efficiency follows approximately a straight line as a function of SNR (measured in dB). In the following, this linear approximation (for a symbol error probability $P_{\mathrm{err}} = 10^{-5}$) is used to distribute bits to individual subcarriers:

$$C'_{\mathrm{QAM}} \approx 0.31 \cdot (10 \lg \frac{S}{N} - 6.7). \tag{7}$$

Especially for low SNRs (2-PSK) Eq. (7) is a significantly better approximation than the "gap approximation" [13, 6]:

$$C'_{\mathrm{gap}} = \mathrm{ld}\left(1 + \frac{S}{N} \cdot \frac{1}{\Gamma}\right) \tag{8}$$

where 10 lg Γ denotes the SNR gap between channel capacity and the bandwidth efficiency of real modulation schemes (approximately 8 dB for $P_{\mathrm{err}} = 10^{-5}$).

In the following, the principle of the bit distribution algorithm for modulator A is described: In a first step, from the given SNRs of the individual subcarriers and the required error probability $P_{\mathrm{err}} = 10^{-5}$, the capacities C'_{QAM_i} are calculated with Eq. (7). These values are rounded to the maximum integers m_i which are smaller than C'_{QAM_i}. If in all subchannels i a number of m_i bits are mapped to complex symbols of corresponding QAM schemes, the error probability is smaller than required. A sum of $m_\Sigma = \sum_i m_i$ bits can be transmitted per OFDM symbol with less than the required error probability.

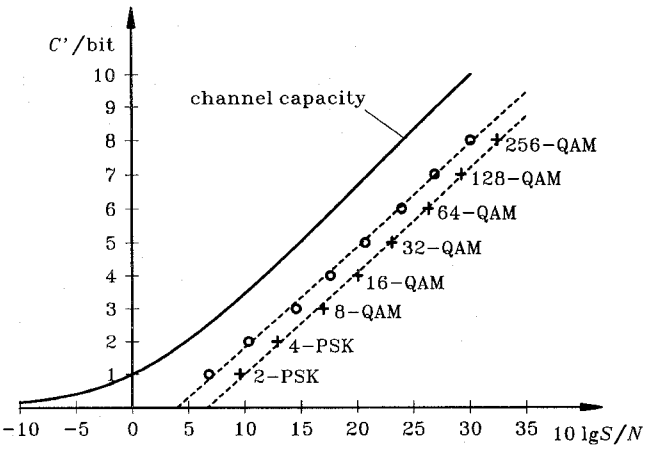

Figure 6: Bandwidth efficiency of different modulation schemes versus SNR for a symbol error probability $P_{\text{err}} = 10^{-3}$ (circles) and $P_{\text{err}} = 10^{-5}$ (crosses).

The required number of bits M per OFDM symbol is determined by the requested service and usually does not depend on time (constant bit rate transmission is assumed). The number of bits m_Σ that can actually be transmitted with the given quality will usually not coincide with the requested number M.

In case the total number of bits m_Σ is smaller than M, the numbers of bits in individual subchannels have to be increased. Of course, with this measure the error probability will increase above the desired one. The additional bits have to be distributed on the subchannels such that the error probability is increased as small as possible. The corresponding algorithm is described in the following: The additional bits are distributed with the target to minimize the maximum difference $m_i - C'_{\text{QAM}_i}$. One (computationally not efficient) method is to add successively bits to subchannels where the difference $m_i - C'_{\text{QAM}_i}$ is minimal.

In case the total number of bits m_Σ is greater than M, the numbers of bits in individual subchannels have to be reduced. With this measure the error probability will decrease below the desired one. The reduction of bits in the subchannels is carried out such that the error probability is decreased as far as possible. This is done by reducing bits with the target to maximize the minimum difference $C'_{\text{QAM}_i} - m_i$. One (computationally not efficient) method is to reduce successively bits at subchannels where the difference $C'_{\text{QAM}_i} - m_i$ is minimal.

For a small SNR the values C'_{QAM_i} can also become negative. This only means that the error probability is usually higher than desired. But nevertheless with the above described algorithm, the distribution of bits is carried out in an optimum way so that the overall error probability becomes minimum. The above described algorithm for modulator A maximizes the minimum (with respect to all subcarriers) SNR margin (difference between actual and desired SNR for a given error probability).

The modulator B optimizes the power spectrum (PSD) and distribution of bits simultaneously. The optimum Hughes-Hartog algorithm [5] which was designed for the twisted-pair channel, cannot be applied since it maximizes the data rate. Because of the temporal fluctuations of the radio channel, the data rate varies with time. Therefore, the Hughes-Hartog algorithm cannot be used for constant bit rate communications.

In the following, the power and bit distribution algorithm of modulator B is described: In a first step, an initial bit distribution is calculated. A possible initial bit distribution is e.g. the result of modulator A for a frequency-independent power distribution. Next, the total required power $\sum P_i$ for the desired error probability is calculated from Eq. (7):

$$P_i = \frac{k\,T_0\,F\,B}{|H(\omega_i)|^2 \cdot n_{\text{FFT}}} \cdot 10^{\left(\frac{m_i}{3.1}+0.67\right)}. \qquad (9)$$

Successively, at each of the subcarriers the number of bits m_i is reduced by one bit (if possible). The reduction of the total required power is calculated for each subcarrier. At the subcarrier with the highest power reduction, the number of bits is reduced by a single bit. Next, successively at each of the subcarriers the number of bits is increased by one bit. The increase of the total required power is calculated for each subcarrier. At the subcarrier with the smallest power increase, the number of bits is increased by a single bit. This procedure of decreasing and increasing the number of bits per subcarrier is repeated until the bit distribution does not change any more. At this point, the optimum bit distribution is found. Simultaneously, the total required power for the desired error probability is minimized.

Finally the (average) power of all subcarriers is adjusted by the same factor $P_x / \sum P_i$ so that the total power equals the available power P_x. The result of this procedure is that the same SNR margin for all subcarriers is achieved. The obtained SNR margin is the maximum possible so that the error probability becomes minimum. Therefore, modulator B calculates the optimum distribution of power and bits.

The results of the optimization processes of both, modulator A and modulator B, are shown in Fig. 7. For comparison, the upper diagram shows the absolute value of the transfer function in dB. The lower diagram shows that for this specific example, both modulators yield the same distribution of bits. Furthermore, the power distribution and SNR is shown for both modulators. The transmit power for modulator B varies within a range of approx. -1.5 dB to 1.5 dB corresponding to the difference of approx. 3 dB between SNRs of adjacent QAM schemes.

4 Simulation results

The simulation was carried out with a complex baseband representation of the signals. No oversampling was used since only linear components (except the detectors) are included in the block diagram. The simulation parameters are summarized in Table 2.

length of FFT interval	256 samples
length of guard interval	25 or 50 samples
HF bandwidth	5 MHz
sampling rate in complex baseband	5 MHz
noise figure of the receiver	6 dB
number of transmitted QAM symbols	5×10^5

Table 2: Simulation parameters.

The temporal location of the FFT interval with respect to the cyclic extension at the receiver (i.e. the time synchronization of the OFDM blocks) is optimized so that the bit error ratio becomes minimum. The simulation results are presented in the following figures. Figures 8 and 9 show the simulated bit

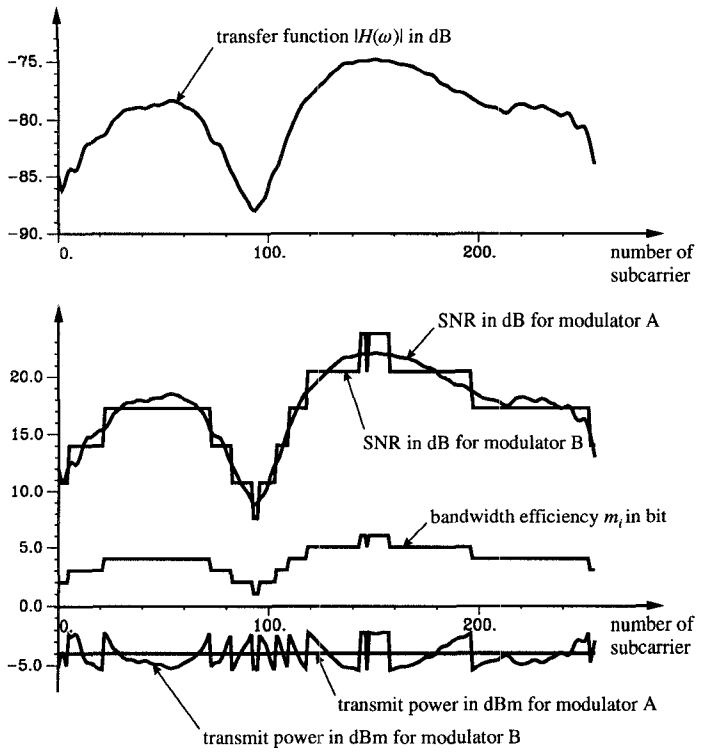

Figure 7: Illustration of adaptive modulation: absolute value of transfer function $|H(\omega)|$, SNR, bandwidth efficiency m_i, and normalized power per OFDM channel. (The average normalized power per subcarrier equals total average power.) Modulator A optimizes only the modulation schemes, modulator B optimizes both, modulation schemes and power distribution.

error ratio as a function of the transmitted power for measurement 1 and 2, respectively.

In particular, for modulation schemes with high bandwidth efficiency an error floor can be noticed in case of insufficient length of the guard interval due to interblock interference. The error floor is reduced or vanishes if the guard interval is extended. Due to the larger delay spread in measurement 2, a higher error floor can be observed. The figures show that fixed OFDM is more sensitive against interblock interference than adaptive OFDM. This can be explained by the fact that in the adaptive system, bad channels are not used or only used with small signal alphabets where a small amount of interblock interference is not so critical.

In the following, the power required for a bit error ratio of 10^{-3} is compared for fixed and adaptive modulation. For a sufficient length of the guard interval a gain due to adaptive modulation of 5 ... 15 dB can be observed for the investigated channels. If a lower bit error ratio is considered, the gain is even higher. Especially for the NLOS channel, the bit error ratio can be reduced dramatically with adaptive OFDM. The loss for using modulator A with frequency-independent PSD instead of modulator B with optimum PSD is less than 1.1 dB. Because of this small loss, it is recommended to use a constant power spectrum in order to save computational or signalling effort.

Finally, the channel capacity is compared with the data rates achievable with optimum adaptive OFDM (modulator B). It is assumed that a bit error probability of 10^{-5} can be tolerated. The results of the comparison are summarized in Table 3. Because of its superior performance, only adaptive modulation is considered. In this table, the loss in data rate due to the cyclic extension (guard interval) is taken into account, whereas the loss due to the signalling for the synchronization of the adaptive modulation is neglected. It can be noticed that the data rate reaches 30 ... 58 % of channel capacity according to Eq. (2). The fraction is smaller than for an AWGN channel because of the time-variant behaviour of the radio channel and the loss for the guard interval. The difference for the NLOS channel is smaller than for the LOS channel, since in the NLOS channel, frequency-selective fluctuations compensate each other to a higher extent. The frac-

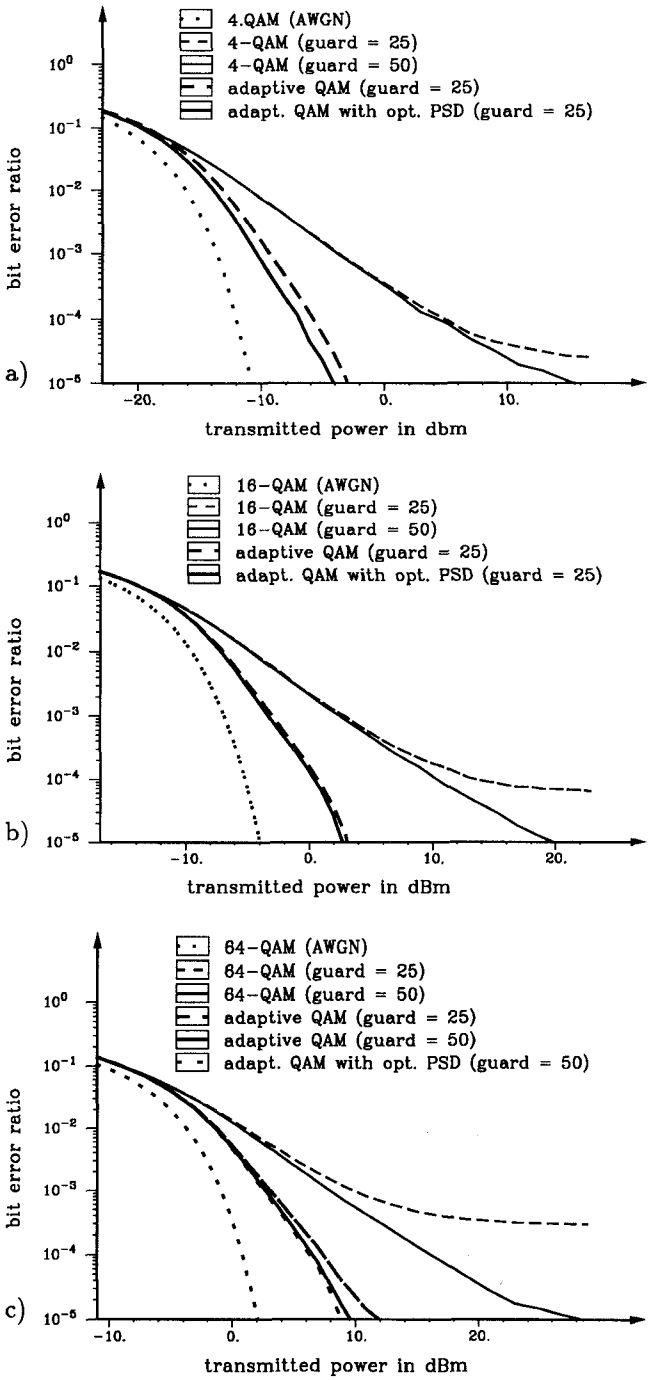

Figure 8: Bit error ratio versus transmitted power with different modulation schemes and guard lengths (measured in samples), radio channel data from measurement 1. Average bandwidth efficiency for all modulation schemes: a) $C' = 2$ bit, b) $C' = 4$ bit, c) $C' = 6$ bit.

DOCKET ALARM

Explore Litigation Insights

Docket Alarm provides insights to develop a more informed litigation strategy and the peace of mind of knowing you're on top of things.

Real-Time Litigation Alerts

Keep your litigation team up-to-date with **real-time alerts** and advanced team management tools built for the enterprise, all while greatly reducing PACER spend.

Our comprehensive service means we can handle Federal, State, and Administrative courts across the country.

Advanced Docket Research

With over 230 million records, Docket Alarm's cloud-native docket research platform finds what other services can't. Coverage includes Federal, State, plus PTAB, TTAB, ITC and NLRB decisions, all in one place.

Identify arguments that have been successful in the past with full text, pinpoint searching. Link to case law cited within any court document via Fastcase.

Analytics At Your Fingertips

Learn what happened the last time a particular judge, opposing counsel or company faced cases similar to yours.

Advanced out-of-the-box PTAB and TTAB analytics are always at your fingertips.

API

Docket Alarm offers a powerful API (application programming interface) to developers that want to integrate case filings into their apps.

LAW FIRMS
Build custom dashboards for your attorneys and clients with live data direct from the court.

Automate many repetitive legal tasks like conflict checks, document management, and marketing.

FINANCIAL INSTITUTIONS
Litigation and bankruptcy checks for companies and debtors.

E-DISCOVERY AND LEGAL VENDORS
Sync your system to PACER to automate legal marketing.